Nitrate addition stimulates microbial decomposition of organic matter in salt marsh sediments

Journal:	*Global Change Biology*
Manuscript ID	GCB-18-0672
Wiley - Manuscript type:	Primary Research Articles
Date Submitted by the Author:	29-Apr-2018

Complete List of Authors:	Bulseco-McKim, Ashley; Northeastern University, Marine and Environmental Sciences Giblin, Anne; Marine Biological Laboratory, The Ecosystems Center Tucker, Jane; Marine Biological Laboratory, The Ecosystems Center Murphy, Anna; Northeastern University, Marine and Environmental Sciences Sanderman, Jonathan; Woods Hole Research Center, Hiller-Bittrolff, Kenly; University of Massachusetts Boston, Biology Department Bowen, Jennifer; Northeastern University, Marine and Environmental Sciences

Keywords:	Nitrate, Decomposition, Organic Matter, Microbes, Anaerobic Respiration, Salt Marsh, Flow Through Reactor, 16S rRNA gene

Abstract:	Salt marshes store carbon at rates that are more than an order of magnitude greater than their terrestrial counterparts, helping to mitigate negative consequences of climate change. As nitrogen loading to coastal waters continues to rise, primarily in the form of nitrate, it is unclear what effect it will have on carbon storage capacity of these highly productive systems. This uncertainty is largely driven by the dual role nitrate can play in biological processes, where it can serve as either a nutrient that stimulates primary production or a powerful electron acceptor fueling heterotrophic metabolism. Here, we used a controlled flow through reactor experiment to test the role of nitrate as an electron acceptor, and its effect on organic matter decomposition and the associated microbial community in salt marsh sediments. We observed a significant increase in organic matter decomposition in response to nitrate and found that this pattern persisted even at sediment depths typically considered to be less labile. Nitrate addition significantly altered the microbial community and decreased alpha diversity, selecting for taxa belonging to groups known to reduce nitrate and oxidize more complex forms of organic matter. Fourier Transform-Infrared Spectroscopy data further supported these results, suggesting that nitrate facilitated decomposition of complex organic matter compounds into more labile forms. Taken together, these results suggest the existence of organic matter pools that only become accessible with nitrate and would otherwise remain stable. The existence of such pools could have important implications for carbon storage, since greater

	decomposition rates may result in less overall burial of organic matter-rich sediment. Given the extent of nitrogen loading along our coastlines, it is imperative that we better understand the resilience of salt marsh systems to nutrient enrichment, especially if we hope to rely on salt marshes, and other blue carbon systems, for long-term carbon storage.

Title Page

Running Head: Nitrate affects organic matter decomposition

Title: Nitrate addition stimulates microbial decomposition of organic matter in salt marsh sediments

List of Authors: Ashley Bulseco-McKim[1], Anne E. Giblin[2], Jane Tucker[2], Anna E. Murphy[1], Jonathan Sanderman[3], Kenly Hiller-Bittrolff[4], and Jennifer L. Bowen[1]*

Institute or laboratory of origin:

[1]Department of Marine and Environmental Sciences, Marine Science Center, Northeastern University, MA 01908.

[2]Ecosystems Center, Marine Biological Laboratory, MA 02543

[3]Woods Hole Research Center, Falmouth, MA 02540

[4]Department of Biology, University of Massachusetts Boston, Boston, MA 02125

Corresponding author:

Jennifer Bowen, Department of Marine and Environmental Sciences, Marine Science Center, Northeastern University, MA 01908, Phone: 617-373-2059, Email: je.bowen@northeastern.edu

Keywords: Nitrate, decomposition, organic matter, microbes, anaerobic respiration, salt marsh, flow through reactor, 16S rRNA gene

Paper Type: Primary Research Article

Abstract

Salt marshes store carbon at rates that are more than an order of magnitude greater than their terrestrial counterparts, helping to mitigate negative consequences of climate change. As nitrogen loading to coastal waters continues to rise, primarily in the form of nitrate, it is unclear what effect it will have on carbon storage capacity of these highly productive systems. This uncertainty is largely driven by the dual role nitrate can play in biological processes, where it can serve as either a nutrient that stimulates primary production or a powerful electron acceptor fueling heterotrophic metabolism. Here, we used a controlled flow through reactor experiment to test the role of nitrate as an electron acceptor, and its effect on organic matter decomposition and the associated microbial community in salt marsh sediments. We observed a significant increase in organic matter decomposition in response to nitrate and found that this pattern persisted even at sediment depths typically considered to be less labile. Nitrate addition significantly altered the microbial community and decreased alpha diversity, selecting for taxa belonging to groups known to reduce nitrate and oxidize more complex forms of organic matter. Fourier Transform-Infrared Spectroscopy data further supported these results, suggesting that nitrate facilitated decomposition of complex organic matter compounds into more labile forms. Taken together, these results suggest the existence of organic matter pools that only become accessible with nitrate and would otherwise remain stable. The existence of such pools could have important implications for carbon storage, since greater decomposition rates may result in less overall burial of organic matter-rich sediment. Given the extent of nitrogen loading along our coastlines, it is imperative that we better understand the resilience of salt marsh systems to nutrient enrichment, especially if we hope to rely on salt marshes, and other blue carbon systems, for long-term carbon storage.

1. Introduction

Carbon dioxide (CO_2) concentrations continue to rise as a result of fossil fuel burning and land-use changes, thereby contributing to increases in global temperature, ocean acidification, and sea level rise. While a number of mitigation strategies have been proposed, recent emphasis has been placed on sequestering CO_2 in blue carbon habitats (Dargusch & Thomas, 2012), which include salt marshes, mangroves, and seagrass meadows (Mcleod et al., 2011; Nelleman et al., 2009). Salt marshes are particularly efficient at storing carbon due to high levels of primary production, the ability to trap organic rich sediments (Chmura et al., 2003), and low rates of microbial decomposition due to largely anaerobic conditions below the first few millimeters of the surface (Reddy & Patrick Jr., 1975). They can bury carbon at a rate more than an order of magnitude greater than that of their terrestrial counterparts, over time scales of thousands of years (Duarte, Middelburg, & Caraco, 2005; Mcleod et al., 2011). As such, they have become a major focus of coastal restoration projects (Macreadie et al., 2017; Warren et al., 2002).

Salt marshes face several anthropogenically-driven threats that can diminish, and potentially reverse, their capacity to store carbon. Here, we focus on the role of coastal nitrogen (N) inputs, which continue to increase in many systems due to fertilizer production, agricultural and urban runoff, enriched groundwater, and atmospheric deposition (Galloway, Leach, Erisman, & Bleeker, 2017). While salt marshes can remove some of this anthropogenic N before entry into the coastal ocean, either by assimilation into plant biomass (Valiela & Teal, 1974) or conversion to gaseous products (NO, N_2, N_2O) via denitrification or anammox (Hopkinson & Giblin, 2008; Kaplan, Valiela, & Teal, 1979; Koop-Jakobsen & Giblin, 2009), it is unclear how much N loading salt marshes can withstand without having negative implications for carbon storage. In general, salt marshes are more resilient to N loading when compared to other coastal systems

because of their ability to efficiently remove N (Valiela & Cole, 2002). There is considerable evidence that nutrient enrichment stimulates aboveground primary production (Kaplan et al., 1979; Morris, Sundareshwar, Nietch, Kjerfve, & Cahoon, 2002; Vivanco, Irvine, & Martiny 2015), which facilitates sediment trapping and marsh accretion (Morris et al., 2002) and augments the carbon sink potential by adding biomass. Other studies have also observed increased belowground production in response to elevated N (Pastore, Megonigal, & Langley, 2017). In some systems, however, responses to N enrichment diminished carbon storage capacity, including lost root biomass, increased belowground microbial respiration, and changes in species composition, all of which can result in lower sediment stability and potential marsh collapse (Langley, Mozdzer, Shepard, Hagerty, & Megonigal, 2013; Deegan et al., 2012). Due to these complexities, the exact response of the marsh carbon storage capacity to increased N loading remains unclear.

One plausible explanation for conflicting observations among marsh fertilization experiments may be the form of N that is applied. Many studies cover small spatial scales and apply N in its reduced form, ammonium (NH_4^+) or urea; although some use a mix of oxidized and reduced forms, ammonium nitrate (NH_4NO_3). In contrast, much of the N delivered to the coastal zone occurs in its oxidized form, nitrate (NO_3^-) (Galloway et al., 2008). In addition to supporting primary production through assimilation by marsh vegetation, benthic microalgae, and phytoplankton, NO_3^- can also serve as an energetically favorable electron acceptor to fuel microbial oxidation of organic matter (OM) through various anaerobic respiration processes, including denitrification (Hamersley & Howes, 2005; Kaplan et al., 1979) and dissimilatory nitrate reduction to ammonium (DNRA; Giblin et al., 2013; Thamdrup & Dalsgaard, 2002). Sulfate (SO_4^{2-}) is another important electron acceptor in salt marsh sediments, accounting for up

to 70-90% of total sediment respiration (Howarth, 1984; Howarth & Teal, 1979) due to its virtually unlimited supply from incoming seawater. However, these two electron acceptors are different thermodynamically in that reducing NO_3^- releases more free energy ($\Delta G°H_2$ = -420 kJ) than reducing SO_4^{2-} ($\Delta G°H_2$ = -98.9 kJ) (Canfield, Thamdrup, & Kristensen, 2005). Increased NO_3^- availability, which is typically limiting in coastal systems (Ryther & Dunstan, 1971), may therefore affect the microorganisms using these resources, and consequently alter the ecosystem functions they mediate.

The mechanisms by which this change in function could occur include: 1) a shift in total microbial community structure to an alternative state better fit for a high NO_3^- environment through change in electron acceptor availability 2) alteration of metabolic capacity of the existing microbial community to N-cycling metabolisms due to high physiological plasticity, or 3) some combination of the two (Allison & Martiny, 2008; Meyer, Lipson, Martin, Schadt, & Schmidt, 2004; Shade et al., 2012). Considering the fundamental role microbes play in carbon decomposition, and more indirectly, long-term carbon storage (Benner, Newell, Maccubbin, & Hodsin, 1984; Falkowski, Fenchel, & Delong, 2008), it is essential that we tease apart which of these mechanisms control microbial and ecosystem response to NO_3^- addition. Regardless of the mechanism, prior studies in salt marsh systems suggest functional responses to NO_3^- do occur (Deegan et al., 2012; Koop-Jakobsen & Giblin, 2010). If additional NO_3^- becomes available in a system where the dominant form of metabolism was SO_4^{2-} reduction, increased NO_3^- reduction could result in increased OM oxidation (Froelich et al., 1979). Further, when compared to SO_4^{2-} reducers, NO_3^- reducers, as well as other microbes adapted to high N environments (Treseder, Kivlin, & Hawkes, 2011) can oxidize more complex forms of OM (Achtnich, Bak, & Conrad, 1995), potentially resulting in decomposition of OM that would have otherwise remained stable.

To better quantify the role of marshes in long-term carbon storage it is critical to understand how these systems respond to increasing NO_3^- concentrations. In this study, we investigate whether NO_3^- addition increases decomposition of salt marsh OM. To explicitly address this question, we implemented a controlled flow through reactor (FTR) experiment, where we exposed salt marsh sediments to elevated levels of NO_3^-. We hypothesized that the addition of NO_3^- would stimulate the decomposition of OM when compared to unamended sediments, and that these experiments would reveal the presence of a "NO_3^- accessible" pool of OM that microbes could only oxidize in the presence of this more favorable electron acceptor. We also examined whether depth and age of OM would play a role in the salt marsh sediment response to NO_3^- addition. Specifically, we hypothesized that there would be little difference in decomposition between the NO_3^- and unamended treatments in shallow sediments, since the OM there would be recently deposited and relatively labile, making it accessible for both SO_4^{2-} and NO_3^- reduction. Further, we hypothesized that there would be an overall decrease in decomposition in deeper sediments, where OM lability decreases and becomes less amenable to microbial oxidation, but that there would be a greater stimulation of decomposition at depth in the NO_3^- treatment compared to the unamended sediments. Lastly, we hypothesized that these changes in metabolic function would result from a shift in the microbial community towards taxa better adapted for high N environments.

2. Materials and methods

2.1 Sample collection

We assessed the effect of NO_3^- on the decomposition of sediment OM of varying ages by collecting samples along a depth gradient from salt marsh sediments located in West Creek, part

of a marsh complex located in Plum Island Sound, MA (42.759 N, 70.891 W). West Creek is a relatively pristine reference site monitored as part of a long-term nutrient enrichment experiment called the TIDE project (Deegan et al., 2007). We collected three replicate cores (5 cm diameter and 30 cm deep) from the tall ecotype of *Spartina alterniflora*, a habitat that floods daily and is underwater approximately 35% of the time (Deegan et al., 2007). We sectioned each core into shallow (0-5 cm), mid (10-15 cm), and deep (20-25 cm) sediments and homogenized sections under anoxic conditions. We chose these depths to include OM of varying quality, ranging from relatively newly deposited OM (shallow), to older OM found both within (mid) and beyond (deep) the rooting zone. Based on accretion rates taken from nearby sites, we can estimate that these sediments range from 50 to 100 years in age (Forbrich, Giblin, & Hopkinson, 2018; Wilson et al., 2014). Before proceeding, we removed as much root material as possible from the homogenized cores. We then split each sectioned depth into a plus-NO_3^- and an unamended treatment (filtered seawater). This resulted in three replicates for each treatment at each depth.

2.2 Flow through reactors and experimental design

The flow-through reactor experimental system (Fig. S1) is a modified version of the system described in Pallud, Meile, Laverman, Abell, & Van Cappellen (2007) and Pallud & Van Cappellen (2006). In contrast to whole-core batch incubations or sediment slurries, flow-through reactors provide biogeochemical rate measurements at steady-state conditions and prevent dissolved metabolic byproducts from accumulating in the system. Each flow-through reactor consists of two Plexiglas® caps that are radially scored for uniform flow, sealed with O-rings to prevent leakage, and has a volume of 31.81 cm^3. We confirmed unilateral, homogenous flow in each reactor using the conservative tracer, bromide, in breakthrough experiments (see

supplemental methods for details and supplemental Table S1 and Fig. S2 for flow property results).

Under anoxic conditions we loaded each reactor with homogenized sediment, and randomly assigned each reactor a treatment, plus-NO_3^- (+NO_3^- in 0.2 µm filtered seawater) or unamended (0.2 µm filtered seawater only, representing natural salt marsh conditions). To prepare the two treatment reservoirs, we filtered (0.2 µm) water collected from Woods Hole, MA, sparged each with N_2 gas for approximately 20 minutes until they reached anoxic conditions, and spiked the NO_3^- reservoir with 500 µmol L^{-1} additional $K^{15}NO_3^-$ (Cambridge Isotope Laboratories, Andover, MA). We initially added 350 µmol L^{-1} for the first 25 days, but since NO_3^- was being fully consumed, we increased the concentration to 500 µmol L^{-1} to ensure it was never limiting. Half of the reactors received the plus-NO_3^- treatment and half received the unamended treatment, both at a targeted flow rate of approximately 0.08 mL min^{-1} (see Table S1 for measured flow rate) using peristaltic pumps rigged with 0.89 mm (inner-diameter) MasterFlex FDA viton tubing (Cole Parmer, IL, USA). We then carried out a 92-day experiment under anoxic conditions in a glove bag flushed with nitrogen. Once the FTRs reached steady state at the 10-day mark, we collected samples from both the reservoirs and the effluent throughout the experiment to measure changes in biogeochemical parameters and to monitor flow rate. To assess changes in OM composition and microbial community structure, we homogenized and aliquoted bulk sediment from the start of the experiment (pre) and from sediment in each reactor at the end of the experiment. We dried bulk sediments overnight at 65ºC before freezing at -20°C, and immediately flash froze additional aliquots of sediments in liquid nitrogen for nucleic acid extraction and stored them at -80°C until further analysis.

2.3 Biogeochemical and OM *analyses*

We collected water samples from both the plus-NO_3^- and the unamended reservoir along with all reactor outflows to measure biogeochemical processes resulting from microbial activity approximately every 10 days. To assess total microbial respiration, we measured dissolved inorganic carbon (DIC; $CO_2 + HCO_3 + CO_3^{2-}$) on an Apollo SciTech AS-C3 DIC analyzer (Newark, DE) following methods in Dickson & Goyet (1994). We measured nitrate + nitrite ($NO_3^- + NO_2^-$) via chemiluminescence on a Teledyne T200 NOx analyzer (Teledyne API, San Diego, CA) following methods outlined in Cox (1980), and measured ammonium (NH_4^+) and sulfide colorimetrically on a Shimadzu 1601 spectrophotometer (Kyoto, Japan) following protocols from Solorzano (1969) and Gilboa-Garber (1971), respectively. To calculate production and consumption rates of each analyte (DIC, NO_3^-, NH_4^+, and sulfide) over time, we calculated the difference in concentration between the inflow (reservoir) and the outflow (effluent), corrected for flow rate in L hr^{-1}, and divided by reactor volume (31.81 cm^{-3}) for each sampling point. Because we were not able to measure changes in SO_4^{2-} due to high seawater concentrations and proportionally minor changes resulting from experimental conditions, we determined that sulfate reduction was occurring through the production of sulfide (HS^-) and calculated total sulfate reduction rates (SRR) by taking the sum of HS^- produced and total S storage measured at the end of the experiment (described below). We also calculated the DIC:NH_4^+ ratio to draw general inferences about OM pools being decomposed based on C:N stoichiometry.

To assess geochemical changes in OM, we dried samples at 65°C and fumed samples with 12N HCl before performing elemental composition analysis (percent carbon and nitrogen) on a Perkin Elmer 2400 Series Elemental Analyzer (Perkin Elmer, Billerica, MA) using

acetinalide as a standard. We dried additional samples at 105°C overnight to obtain water content and used these data to calculate bulk density of each reactor assuming a volume of 31.81 cm^3. Lastly, we obtained percent sulfur (%S) by combusting dried samples at 1350°C and measuring sulfur dioxide (SO_2) production on a LECO S635 S analyzer (LECO Corporation, Saint Joseph, MI).

To further characterize changes in OM as a result of NO_3^- addition, we used Fourier-Transform-Infrared Spectroscopy (FT-IR), a technique that provides rapid, detailed information about the relative abundance of chemical functional groups. To prepare samples for FT-IR analysis, we finely ground sediment dried at 40°C for 48 hours. We ran each sample on a Bruker Vertex 70 Fourier Transform Infrared Spectrometer (Bruker Optics Inc., Billerica, MA) outfitted with a Pike AutoDiff diffuse reflectance Accessory (Pike Technologies, Madison, WI) and obtained data as pseudo-absorbance (log[1/reflectance]) in diffuse reflectance mode. We collected at a 2 cm^{-1} resolution with 60 co-added scans per spectrum at the mid-IR range, from 4000-400 cm^{-1}, using a mirror for background correction. Resulting raw spectra were transformed using a calculated two-point linear tangential baseline using Unscrambler X (Camo Software, version 10.1, Woodbridge, NJ) and then assigned peaks according to Margenot, Calderón, Boweles, Parikh, & Jackson (2015) and Parikh, Goyne, Margenot, Mukome, & Calderón (2014).

2.4 Nucleic acid extraction, amplification, and amplicon sequencing

We extracted genomic DNA from approximately 0.25 g wet sediment using the MoBio® PowerSoil DNA Isolation Kit (MoBio Technologies, CA, USA) following manufacturer's instructions, and eluted the DNA into a 35 µL final volume. We amplified in triplicate the V4

region of the 16S rRNA gene using the general bacterial primer-pair 515F (5'-GTGCCAGCMGCCGCGGTAA-3') and 806R (5'-GGACTACHVGGGTWTCTAAT-3') (Caporaso et al., 2011) with Illumina adaptors (Caporaso et al., 2012) and individual 12-bp GoLay barcodes on the reverse primer, using the following reaction: 10 µl 5-Prime Hot Master Mix (Quanta Bio, Beverly, MA), 0.25 µl of 20 µM forward and reverse primers, 13.5 µL DEPC-treated water, and 1 µl of DNA template. PCR cycling conditions follow those outlined by the Earth Microbiome Project (Caporaso et al., 2011). While we acknowledge the bias of these primers against the SAR11 group (Apprill, McNally, Parsons, & Weber, 2015), these bacterioplankton are aerobic (Giovannoni, 2017), and should not play a large role in the microbial community associated with our anoxic experimental conditions. Prior to sequencing, we gel-purified the pooled PCR product using a Qiagen® QIAquick gel purification kit (Qiagen, Valencia, CA) and quantified the resulting purified product using a Qubit® 3.0 fluorometer (Life Technologies, Thermo Fisher Scientific, Waltham, MA). After pooling to equimolar concentrations, we performed sequencing on the Illumina MiSeq (Illumina, San Diego, CA) platform using a 300-cycle kit and V2 chemistry. All reads are deposited in the NCBI Sequence Read Archive under accession number TBD.

2.5 Statistical analyses

To investigate changes in DIC production over time, we performed a linear regression on each core using time as the explanatory variable. We integrated between sampling points to calculate the cumulative flux across the length of the experiment and tested for significant differences in DIC, NH_4^+ production, sulfur storage, and total SO_4^{2-} reduction, as a function of treatment and depth using a two-way ANOVA. For both NO_3^- consumption and sulfide

production, both of which were only detectable in one of the two treatments, we assessed differences among depths using a one-way ANOVA. To account for differences in bulk carbon supply on DIC production, we also calculated total carbon loss by taking the proportion of carbon released as DIC divided by the total mass of carbon per reactor using sediment characteristic data (e.g. water content and %C).

Table 1. Functional group assignments based on Parikh et al. (2014) and modified from Margenot et al. (2015) to evaluate FT-IR spectra using Index II metric. ν = stretching vibration; ν_{as} = asymmetric stretching vibration; ν_s = symmetric stretching vibration; δ = bending vibration.

Band (cm^{-1})	Assignment
3400	ν(N-H), ν(O-H)
2924	aliphatic ν_{as}(C-H)
2850	aliphatic ν_s(C-H)
1650	aromatic ν(C = C)
1470	aliphatic δ(C-H)
1405	aliphatic δ(C-H)
1270	phenol ν_{as}(C-O), carboxylic acid ν(C-O)
1110	polysaccharide ν_s(C-O)
1080	polysaccharide ν_s(C-O)
920	aromatic δ(C-H)
840	aromatic δ(C-H), less substituted

To assess changes in %C, %N, bulk density, and %S throughout the experiment, we calculated the difference between initial and final sediments per core and compared these relative changes among treatment and depth using a two-way ANOVA. We performed principal coordinate analysis (PCoA) across the entirety of the FT-IR spectra and used a PERMANOVA with 999 permutations to test for significant differences by treatment and depth using Manhattan distance to construct the resemblance matrix from the FT-IR data. To further visualize trends in

these data, we also plotted the Pearson's correlation coefficients against wavenumber to determine which spectral bands best explained the distribution of sample scores in the PCoA based on functional group assignments in Table 1. Lastly, we calculated a relative recalcitrance index according to the following equation:

Eq. 1

$$\text{Index II} = \frac{2924 + 2850 + 1650 + 1470 + 1405 + 920 + 840}{3400 + 1270 + 1110 + 1080}$$

where each value represents a wavenumber (Table 1) corresponding to either a carbon (numerator) or oxygen-bonded (denominator) functional group. Higher Index II values are typically associated with greater OM recalcitrance (Ding, Novak, Amarasiriwardena, Hunt, & Xing, 2002; Veum, Goyne, Kremer, Miles, & Sudduth, 2014). We used a two-way ANOVA to compare Index II values to infer relative recalcitrance as a function of treatment and depth.

To investigate bacterial community composition, we analyzed sequence data in QIIME 2 (version 2017.12). We demultiplexed a total of 1,521,493 16S rRNA gene sequences across all samples and inferred amplicon sequence variants (ASVs) using the DADA2 plugin (Callahan et al., 2016) with a maxEE of 2 and the consensus chimera removal method. Quality filtering resulted in an average of 37,381 (± 6,693) sequences per sample. We then assigned taxonomy with the Greengenes 16S rRNA sequence database (version 13-8; McDonald et al., 2012) and removed ASVs occurring only once (singletons) and any sequences matching chloroplasts and mitochondria. After aligning sequences using MAFFT v7 (Katoh & Standley, 2013), we performed beta diversity analysis with weighted UniFrac (Lozupone, lladser, Knights, Stombaugh, & Knight, 2011) on ASV tables normalized to 22,999 sequences (which was our lowest sequencing depth), and tested for significant differences among treatments and depth using PERMANOVA with 999 permutations. To examine within sample diversity, we calculated

a Shannon diversity index with these normalized data and tested for differences across treatment and depth using a two-way ANOVA. We ran a random forest model from the randomForest R package (v4.6-12; Liaw & Wiener, 2002) using 10,000 trees on a filtered feature table containing ASVs present at least 100 times (186 ASVs total) to identify taxa most important in classifying between plus-NO_3^- and unamended treatments, and confirmed model results by examining the out-of-bag error rate (a method that uses bootstrap aggregation to assess performance without a training set) and leave-one-out cross-validation with 999 permutations in the caret R package (v6.0-73; Kuhn, 2016). We conducted all other statistical analyses in R (R Core Team 2012) and used an alpha of 0.05 for all significance testing.

3. Results

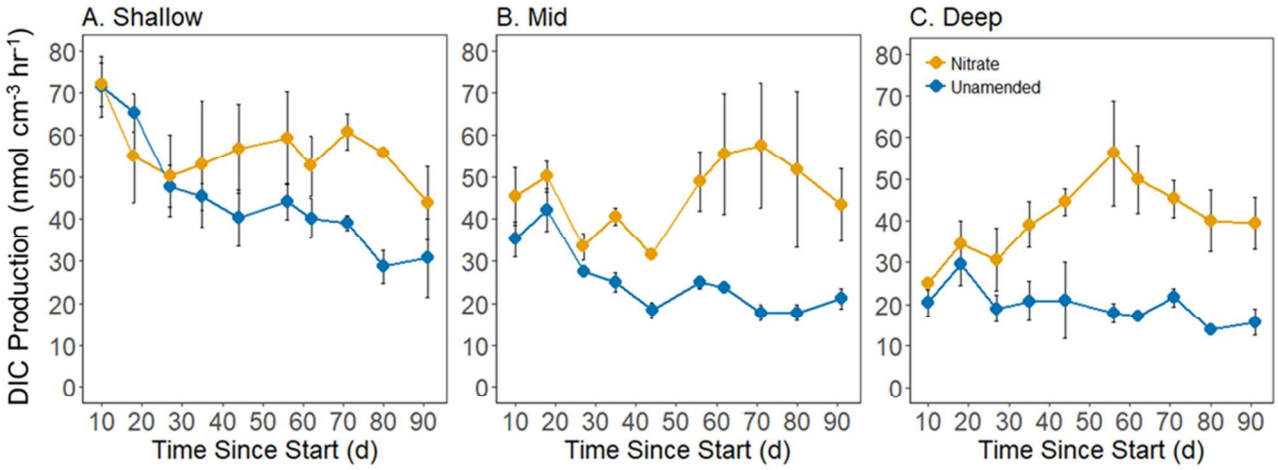

3.1 Biogeochemical rates

Fig. 1. Average (±SE) dissolved inorganic carbon (DIC) production over time (days) across three depths that correspond to different ages of marsh organic matter (panels A-C; n = 3).

Across all depths, the addition of NO_3^- resulted in higher DIC production rates (microbial respiration; Fig. 1) and total cumulative production (Fig. 2) compared to the unamended treatment, both over time and at the end of the experiment. In both treatments, total DIC production decreased with depth (Fig. 2), with shallow sediments exhibiting significantly greater microbial respiration than mid and deep sediments. While DIC production rates decreased over the duration of the experiment in the shallow, unamended sediments (linear regression; p=0.002, $F_{(1,18)} = 12.87$, $R^2 = 0.38$), no such pattern existed in the plus-NO_3^- treatment.

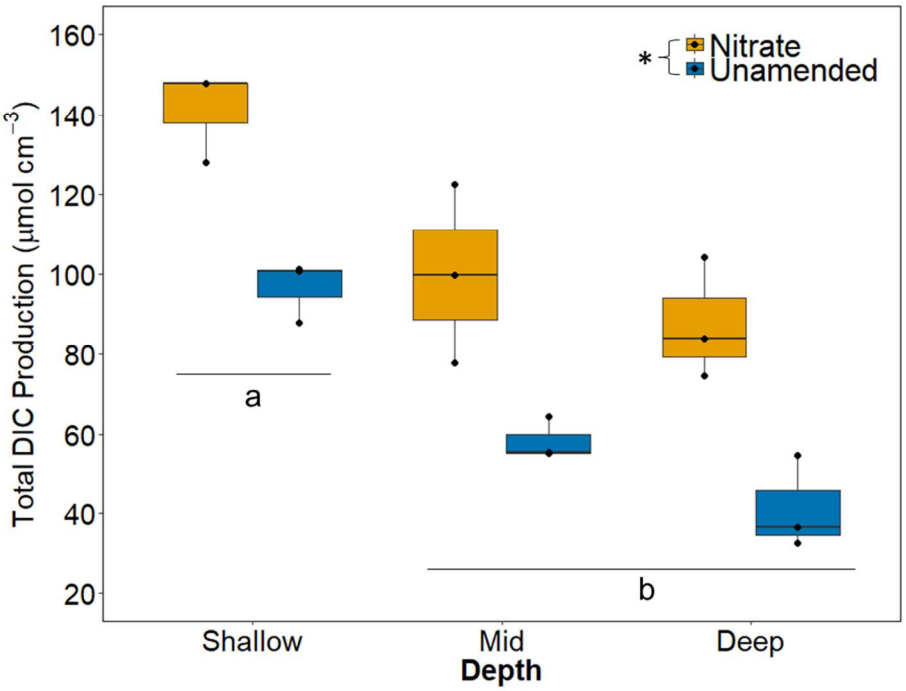

Fig. 2. Average (± SE) cumulative dissolved inorganic carbon (DIC) production in µmol cm-3 for nitrate and unamended treatments at each depth. Boxes represent 25% to 75% quartiles. The solid black line is the median value, and the whiskers are upper and lower extremes. Black dots represent values for each individual reactor. A Two-way ANOVA indicates a significant effect of treatment ($p<0.001$, $F(1,14)=21.73$) and depth ($p<0.001$, $F(2,14)=48.33$) on total DIC production, but there was no significant interaction between the two. Letters represent

300 statistically different DIC production by depth from a Tukey's HSD test corrected for multiple
301 comparisons test and asterisks indicate a significant difference between treatments.
302
303 We measured NO_3^- consumption and sulfide production in reactor effluent (plus total S in
304 sediment) to assess nitrate reduction rates (NRR) and sulfate reduction rates (SRR), respectively.
305 Background NO_3^- concentrations in the incoming seawater were consistently low (0.6-1.2 µM).
306 Although all of this nitrate was reduced throughout the experiment in the unamended treatment
307 the low initial NO_3^- resulted in negligible NRR. In the plus-NO_3^- treatments, NRR ranged from
308 13.9-87.2 µmol cm^{-3}, accounting for 67.1% ± 6.8, 98.2% ± 9.6, and 93.0% ± 10.8 of DIC
309 production in shallow, mid, and deep sediments respectively. There was not a significant
310 difference in total NRR with depth (Fig. 3), which is in contrast to total DIC production, where
311 rates were highest in shallow sediments (Fig. 2).

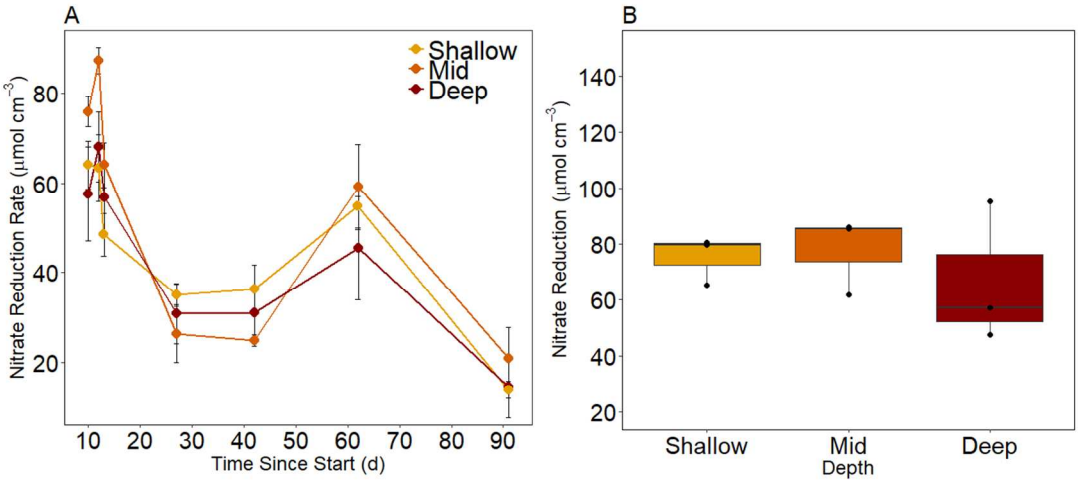

312

313 **Fig. 3. (A)** Average (±SE) nitrate reduction rates over time (days) and **(B)** total nitrate reduction
314 at each depth in the nitrate amended treatment (nitrate was below detection in the unamended
315 sediments. One-way ANOVA indicated no significant difference in nitrate reduction as a
316 function of depth.

Sulfide was undetectable in the plus-NO_3^- treatment but in the unamended treatment sulfide production occurred at all depths (Fig. 4A) and was significantly higher in shallow sediments compared to deep sediments (Fig. 4B). We did observe SRR in both treatments when taking both sulfide and S storage (Fig. 4B,C) into account. In the unamended treatment, SRR accounted for 76.8% ± 1.4, 64.2% ± 9.3, and 59% ± 30.8 of total DIC production in shallow, mid, and deep sediments respectively, and when combined with NRR in the plus-NO_3^- treatment, resulted in 78.1% ± 10.6, 109% ± 13.2, and 98.7% ± 16.4 of total DIC production. There was a significant interaction between treatment and depth on sulfate reduction, with the unamended treatment exhibiting more sulfate reduction than the plus-NO_3^- treatment in shallow sediments, and unamended shallow sediments exhibiting more sulfate reduction than the unamended deep sediments (Fig. 4D).

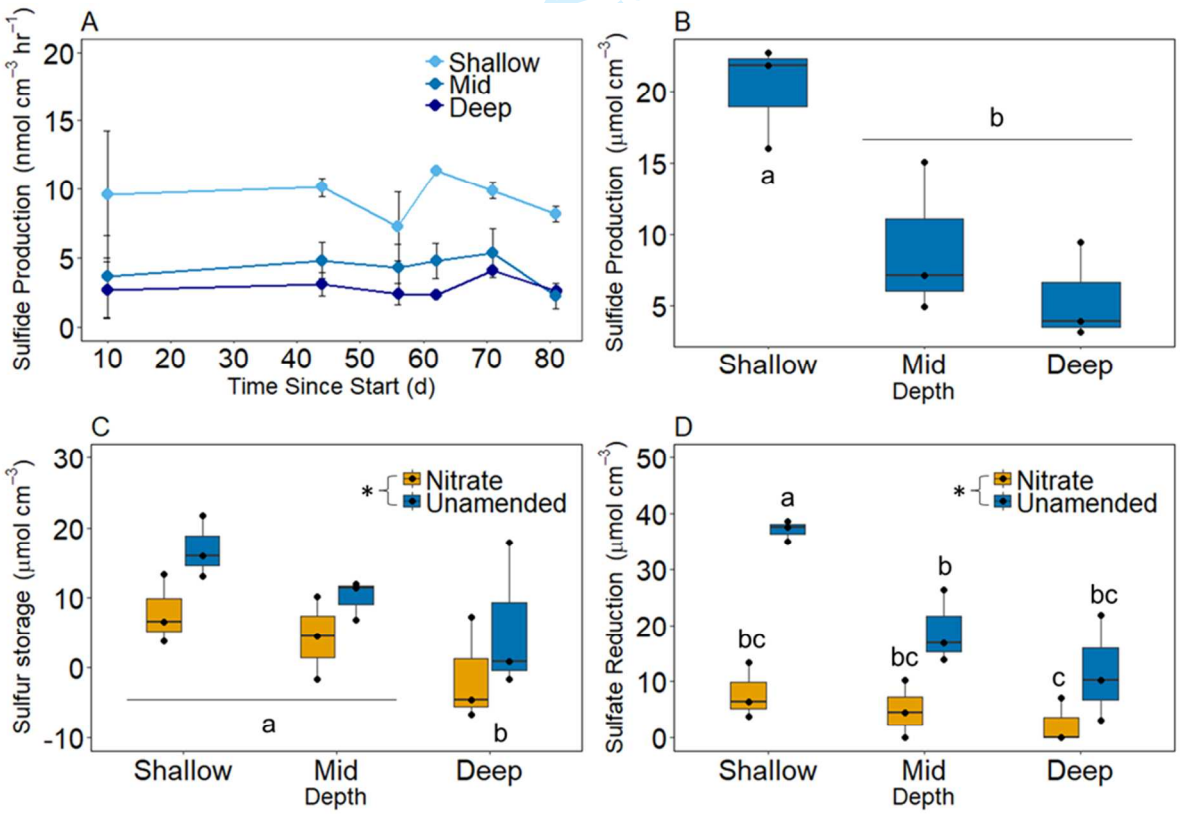

Fig. 4. (A) Average (±SE) sulfide production rates over time (days) and **(B)** total sulfide production. One-way ANOVA indicated shallow sediments exhibited significantly greater sulfide production than mid and deep sediments (p=0.0124, $F_{2,6}$=9.96). **(C)** A two-way ANOVA indicated that total sulfur storage was greater in the unamended treatment across all depths (as indicated by an asterisk; p=0.0243, $F_{1,14}$=7.637), with mid sediments exhibiting higher rates than the shallow and deep sediments (p=0.0367, $F_{2,14}$=4.214). **(D)** There was a significant interaction between treatment and depth on total sulfate reduction (sulfide + sulfur production) (p=0.029, $F_{2,12}$=4.806). Letters represent statistically different sulfate reduction from a Tukey's HSD test corrected for multiple comparisons test.

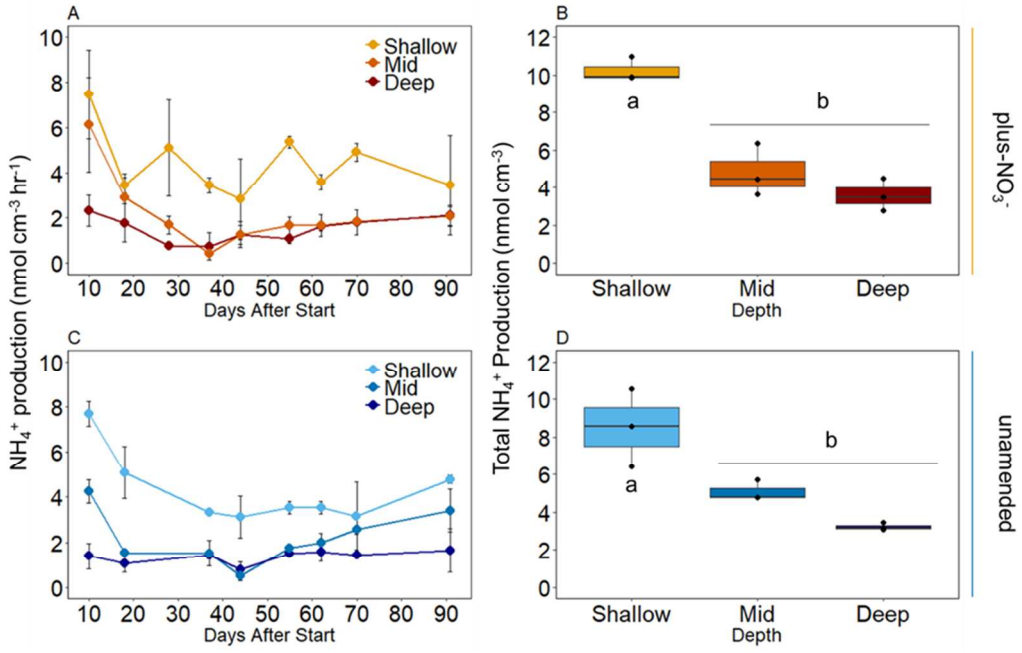

Fig. 5. Average (±SE) ammonium production rates over time (days) in the nitrate **(A)** and unamended **(C)** treatments, and total ammonium production in µmol cm^{-3} across depth for nitrate **(B)** and unamended **(D)** treatments. While there was no effect of treatment, a one-way ANOVA indicated a significant effect of depth (nitrate: p<0.001, $F_{2,6}$=37.47; unamended: p=0.005, $F_{2,6}$=14.09), as indicated by a Tukey's HSD test corrected for multiple comparisons.

While there was no significant difference in NH_4^+ production between treatments, shallow sediments produced significantly more NH_4^+ when compared to mid and deep sediments in both the plus-NO_3^- and unamended treatments (Fig. 5). In addition, the DIC:NH_4^+ ratio was significantly higher in the plus-NO_3^- treatment, while the unamended treatment remained consistently low across all depths (Fig. 6) and was similar to the C:N value of sediments from the start of the experiment (13.66 ± 0.69).

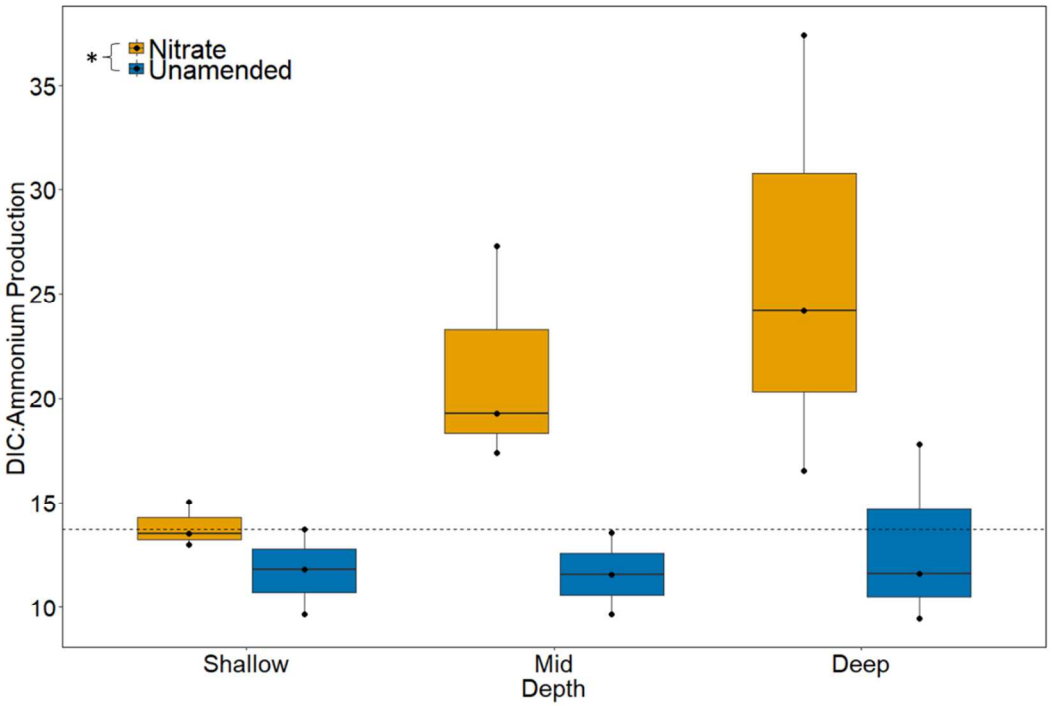

Fig. 6. The ratio of DIC to ammonium production calculated per core was greater in the plus-NO_3^- treatment when compared to unamended sediments, while depth was insignificant, according to a two-way ANOVA (p=0.007, $F_{1,14}$=10.11). The dotted line indicates the average C:N ratio of sediments from this experiment (13.66 ± 0.69).

355 **Table 2.** Average (±SE) bulk density, change in carbon (mg), nitrogen (mg), and sulfur (mg), and final molar C:N per reactor (N=3
356 per treatment-depth combination). Two-way ANOVA indicates a significant difference in nitrogen lost among depths (p=0.00169,
357 $F_{2,14}$=10.417) but not between treatments, and a significant increase in total S in the unamended treatment (p=0.018, $F_{1,12}$ = 7.365)
358 compared to the plus- NO_3^- treatment. Letters represent results from Tukey's HSD test corrected for multiple comparisons.

	Bulk Density	Δ Carbon (mg)	Δ Nitrogen (mg)	Molar C:N	Δ Sulfur (mg)
Unamended					
Shallow	0.22 (0.01)	-141.42 (51.71)	-13.76 (1.2)^{a}	13.24 (0.10)	63.7 (9.99)^{a}
Mid	0.21 (0.01)	-34.69 (13.56)	-6.38 (1.66)^{b}	13.97 (0.27)	39.22 (6.98)^{ab}
Deep	0.22 (0.02)	-41.29 (36.94)	-3.35 (1.24)^{b}	14.17 (0.18)	19.24 (21.15)^{ab}
Nitrate					
Shallow	0.24 (0.02)	-154.12 (60.93)	-13.32 (1.65)^{a}	13.10 (0.09)	25.28 (9.63)^{ab}
Mid	0.22 (0.02)	-91.49 (60.93)	-8.39 (3.90)^{b}	13.71 (0.09)	14.98 (11.38)^{ab}
Deep	0.24 (0.01)	-76.12 (27.05)	-5.55 (2.04)^{b}	14.10 (0.20)	-4.89 (14.31)^{b}

359 *3.2 Organic matter*

360 We compared change in carbon, N, molar C:N, and S in the plus-NO_3^- and unamended
361 sediments versus sediments collected prior to the experiment (Table 2). There was no significant
362 difference in pre- versus post-experiment carbon or molar C:N between treatments; however,
363 there was a change in N by depth and total S by depth and treatment, with significantly greater S
364 concentrations in the unamended sediments (Fig. 4C).

365 The proportion of carbon lost as DIC throughout the experiment ranged only from 0.76 to
366 3.47% of the total carbon in each reactor, so it is not surprising that we did not detect significant
367 changes in most bulk sediment properties between treatments. To observe more precise changes
368 in OM, we applied FT-IR spectroscopy and explored relative shifts in chemical functional groups
369 related to decomposition processes. A principal coordinates analysis (PCoA; Fig. 7A) of the
370 whole FT-IR spectra using Manhattan distances indicated separation by depth along the first
371 coordinate axis (explaining 77.6% of the variance) and treatment along the second coordinate
372 axis (explaining 22.2% of the variance), both of which were significant according to
373 PERMANOVA analysis (Fig. 7A). Pairwise comparisons of mean Manhattan distances further
374 indicated that each depth was significantly different from the rest (shallow-mid, p=0.006,
375 t=3.0287; mid-deep, p=0.009, t=2.7155; shallow-deep, p=0.001, t=5.9444), but when examining
376 treatment, only pre- and unamended sediments were significantly different from each other
377 (p=0.019, t=2.1981). We next plotted the Pearson's correlation coefficient against wavenumber,
378 which accounted for 99.8% of total variance in the PCoA. This allowed us to identify absorbance
379 peaks that were most responsible for distinguishing among sample groups (Fig. 7B). The
380 functional groups that exhibited the most influence on separation included lignin-like compounds
381 at 840 and 1650 cm^{-1} (Artz et al., 2008), polysaccharides at 1080 cm^{-1}, and aliphatic carbon at

382 1470 cm^{-1} (Parikh *at al.*, 2014). Index II, which allows for inferences about sample recalcitrance,
383 was significantly greater in both the plus-NO_3^- and unamended treatments post incubation when
384 compared to initial sediments; however, there was no difference between the plus-NO_3^- and
385 unamended treatments at the end of experiment and no difference by depth (Fig. 7C).

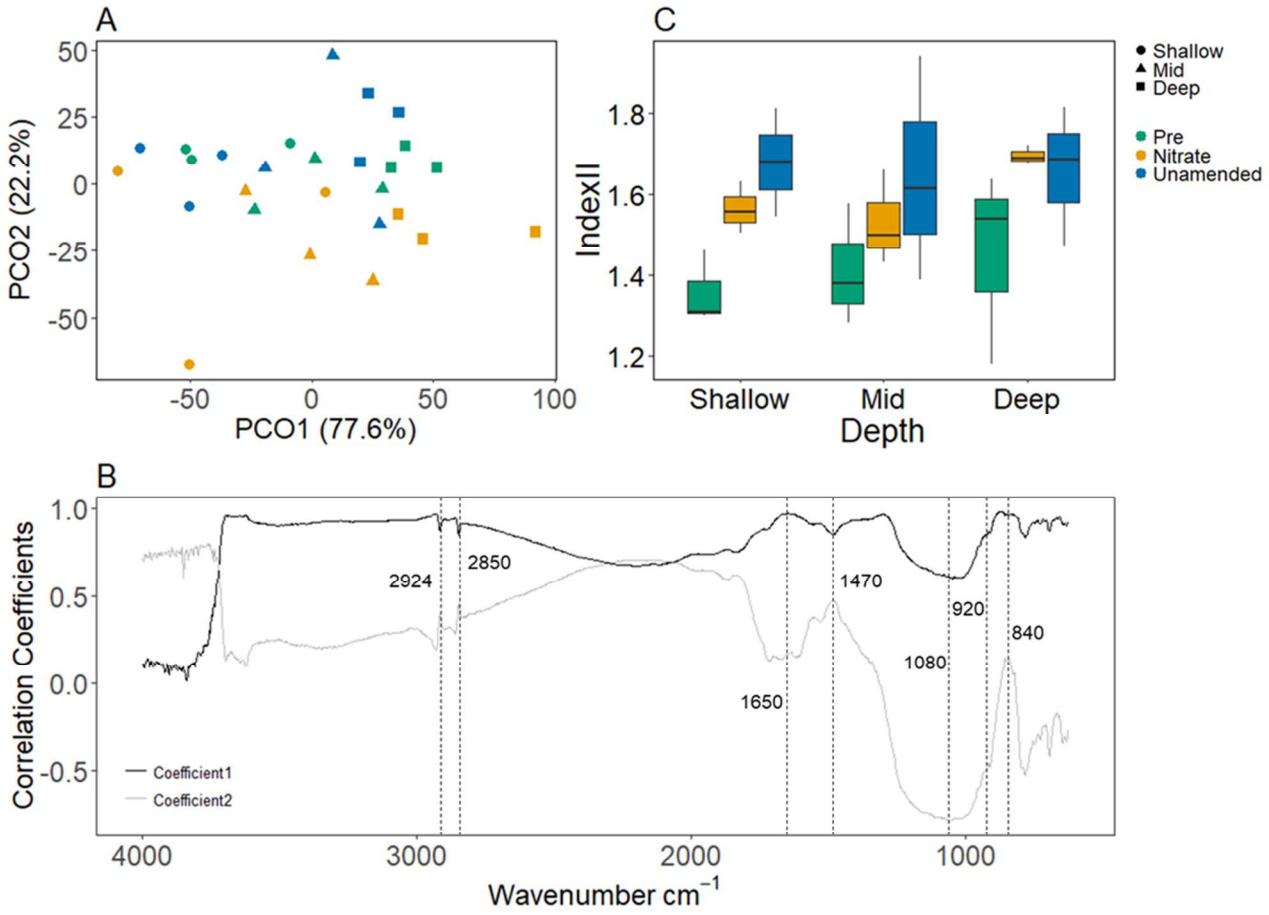

386

387 **Fig. 7. (A)** Principal coordinates analysis (PCoA) of Fourier Transform-Infrared Spectra (FT-IR)
388 indicates significant differences by treatment (PERMANOVA; p=0.017, $F_{2,18}$ = 3.314) and depth
389 (p=0.001 $F_{2,18}$ = 16.598). **(B)** Pearson's correlation coefficients plotted against wavenumber
390 representing regions most discriminating across two axes shown in A. Dotted lines indicate
391 functional group assignments listed in Table 1, with 840-920 and 1650 cm^{-1}= aromatic carbon
392 and lignin-type signatures, 1080 cm^{-1} = polysaccharides, and 2850-2924 cm^{-1} = aliphatic carbon.
393 **(C)** A two-way ANOVA of Index II values (eq. 1) indicated a significant effect of treatment but

not depth, with a higher recalcitrance index in plus-NO_3^- and unamended treatments when compared to initial sediments.

3.3 Microbial community composition in response to nitrate

A principal coordinates analysis constructed from Weighted UniFrac analysis revealed a significant effect of both treatment and depth on microbial community composition (Fig. 8A). There was a clear separation in community similarity along the primary axis (43.20% of the variance explained) due to NO_3^- addition, and a separation driven primarily by differences between shallow and mid/deep sediments (Fig. 8A) along the secondary axis (20.82% of the variance explained). To determine the effect of NO_3^- addition on alpha diversity, we calculated the Shannon Index and found a significant effect of both treatment and depth, but not the interaction of the two factors. Across all depths, alpha diversity was significantly lower in the plus-NO_3^- treatment when compared to the unamended treatment (Fig. 8B).

A random forest model, using 10,000 trees and 186 predictor variables derived from the most abundant ASVs, correctly classified microbial communities as belonging to either the plus-NO_3^- or unamended treatment 100% of the time with a 0% out-of-bag error rate. Leave-one-out cross-validation confirmed model performance, with a Cohen's kappa statistic of 100%, which compares observed accuracy to expected accuracy due to random chance. The top 30 ASVs most important in discriminating between treatments accounted for 45.2% of total sequences and included taxa from Phyla Bacteroidetes, Proteobacteria, Chlorobi, Caldithrix, Chloroflexi, Planctomycetes, Acidobacteria, Gemmatimonadetes, Verrucomicrobia, and candidate group WWE1 (Table S2; Fig. 9). Out of these 30 ASVs, classes from Flavobacteria, Gammaproteobacteria, Alphaproteobacteria, and Ignavibacteria were more abundant in the plus-NO_3^- treatment, while the unamended treatment was much more diverse, including classes from

418 Deltaproteobacteria, Bacteroidia, Caldithrix, Anaerolineae, Cloacamonae, BPC102, Gemm-2,
419 Phycisphaerae, Epsilonproteobacteria, Alphaproteobacteria, Verrucomicrobiae, and
420 Betaproteobacteria. We also tested the random forest model without excluding rare taxa (but still
421 removing singletons) to see if these rarer ASVs would have a disproportionate influence on the
422 dataset. This also resulted in 100% classification rate and 0% out-of-bag error, but only
423 accounted for an additional 1.9% of all sequences (ASVs 31-41 listed in Table S1).

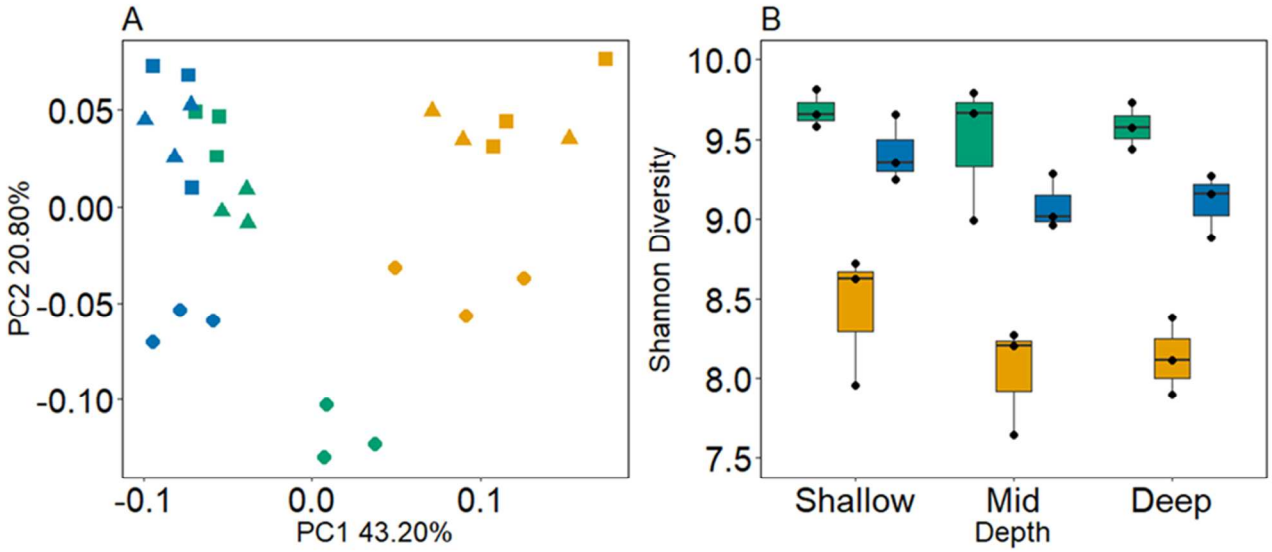

424

425 **Fig. 8. (A)** Principal coordinates analysis constructed based on weighted UniFrac for pre-
426 experiment (green), nitrate (yellow), and unamended (blue) sediments. Shape indicates sample
427 depth: shallow (circle), mid (triangle), and deep (square). Results from a PERMANOVA indicate
428 significant differences in community composition by treatment (p=0.001, $F_{(2,22)}$=11.1095) and
429 by depth (p=0.006, $F_{(2,22)}$=3.0287). **(B)** Shannon diversity index. A two-way ANOVA revealed a
430 significant effect of both treatment (p<0.001, $F_{(2,22)}$=71.207) and depth (p=0.044, $F_{(2,22)}$=3.613),
431 as indicated by a Tukey's HSD test corrected for multiple comparisons, but no effect of the
432 interaction between the two.

433

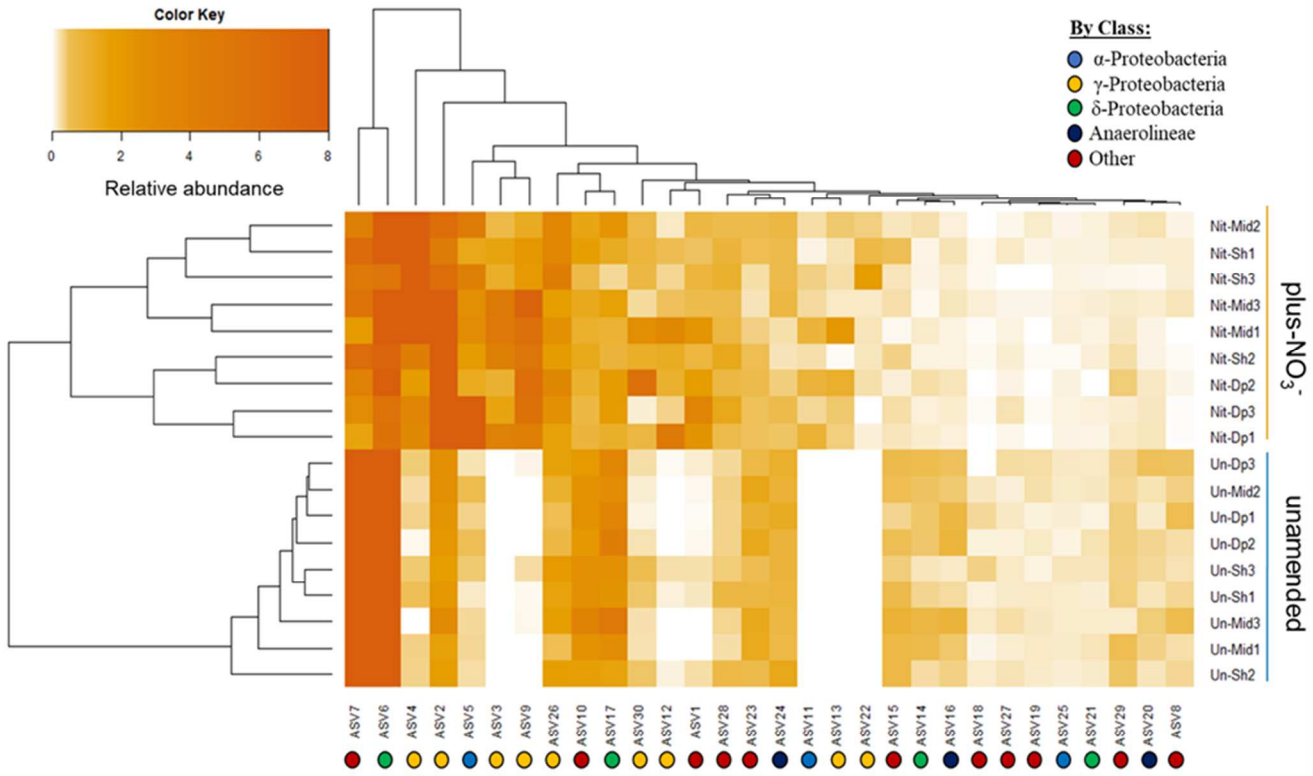

Fig. 9. Heatmap showing relative abundance of top 30 ASVs (45.2% of sequences) most important in correctly discriminating between plus-NO_3^- (top 9 rows) and unamended treatments (bottom 9 rows) according to a random forest classification model. Lighter colors indicate less abundant taxa, while darker colors indicate more abundant taxa. Colored circles represent the taxonomic class of each ASV. Additional taxonomic information can be found in Supplemental Table S2.

4. Discussion

4.1 DIC production rates decreased with depth

Our study used a controlled FTR experiment to test the effect of OM quality and NO_3^- addition on microbial respiration. We found that DIC production decreased as a function of

447 depth, with shallow sediments exhibiting significantly greater microbial respiration rates than
448 mid and deep sediments (Fig. 2). This pattern was particularly evident in the unamended
449 treatment, where DIC production also decreased throughout the duration of the experiment in the
450 shallow sediments (Fig. 1A). The effect of depth on overall DIC production is likely due to
451 changes in OM lability. Surface sediments consist largely of freshly produced organic biomass
452 that is typically more labile (Canfield et al., 2005). Microbes preferentially oxidize these
453 biologically labile compounds first, because the process is less energetically demanding (Hedges
454 et al., 2000); the more refractory compounds that remain are buried into accreting sediment.
455 While microbes can still degrade these less labile organic compounds at depth, it occurs at a
456 much slower rate (Westrich & Berner, 1984), resulting in decreased decomposition. Initial bulk
457 sediment carbon and molar C:N in this experiment did not differ significantly among the
458 different depths (Table 1); although the FT-IR spectra indicated a significant difference in
459 functional groups (Fig. 7A) at different depths driven primarily by polysaccharide depletion (Fig.
460 7B), which suggests decreasing lability in deeper sediments.

461 This pattern is also, in part, due to decreasing availability of powerful electron acceptors
462 in anoxic marsh sediments. Energetically-favorable electron acceptors, such as NO_3^-, are
463 preferentially reduced at the surface and are therefore depleted in deeper sediments (Canfield et
464 al., 2005). While SO_4^{2-} is rarely limiting in most marsh systems due to it high concentration in
465 seawater and delivery via incoming tides (Howarth & Teal, 1979; Jorgensen, 1977), SO_4^{2-}
466 reduction is a much less energetically favorable metabolic pathway, releasing less free energy
467 per mole of carbon oxidized compared to NO_3^- reduction. Since there is less energy available to
468 degrade OM that has accumulated with time, rates of decomposition generally decrease with
469 depth (Arndt et al. 2013; Canfield et al., 2005); though the presence of roots and bioturbation can

alter this pattern (Aller & Aller, 1998; Canfield & Farquhar, 2009; Kostka et al., 2002). This is consistent with the decrease in DIC production (Fig. 2) and sulfide production (Fig. 4B) we observed in the deeper unamended sediments. Further, DIC production decreased as a function of time in the surface unamended treatment (Fig. 1), suggesting that after first oxidizing the more labile OM compounds, only more recalcitrant, less available OM remained, leading to decreased decomposition rates. This result corroborates other studies that find a strong relationship between OM degradability and SRR, with decreasing OM lability resulting in lower decomposition rates regardless of SO_4^{2-} availability (Canfield, 1989; Westrich & Berner, 1984).

4.2 Evidence for a nitrate accessible pool of OM

The addition of NO_3^- resulted in significantly greater DIC production across all depths, most notably in deeper sediments, where OM is older and less labile. While NO_3^- is a powerful terminal electron acceptor that fuels high rates of denitrification and DNRA in salt marshes, it is typically coupled with nitrification at oxic interfaces or rooting zones (Hamersley & Howes, 2005; Howes, Howarth, Teal, & Valiela, 1981), and hence limited at depth where it cannot be internally regenerated. By experimentally adding NO_3^- here, similar to what might occur in coastal environments under high N loading, we thereby increased NO_3^- availability. In doing so, we increased rates of NO_3^- reduction (Fig. 3) and OM oxidation (Fig. 1-2), and consequently increased rates of decomposition. These results suggest the existence of a "NO_3^--accessible" OM pool and emphasize that the definition of "recalcitrant" can differ depending on both OM lability and electron acceptor availability. OM that is considered recalcitrant under SO_4^{2-}-only conditions may no longer be stable under NO_3^- availability.

High NO_3^- conditions may stimulate the microbial community to break down these otherwise stable, less labile OM compounds by providing more energy for metabolic processes. Higher DIC:NH_4^+ ratios in the plus-NO_3^- treatment provide support for this claim. In general, more DIC relative to NH_4^+ production indicates that microbes are using OM with higher C:N values (Canfield et al., 2005). In the plus-NO_3^- treatment, particularly at depth, the DIC:NH_4^+ ratio was much higher, suggesting that microbial communities may be accessing a different OM pool compared to unamended sediments, which remained consistently low and very similar to the average sediment C:N ratio from the start of the experiment (Fig. 5). It is noteworthy that the ratio of DIC:NH_4^+ in the plus-NO_3^- and unamended treatment were similar in shallow sediments, where OM is more labile and appears to be accessible to both NO_3^- and SO_4^{2-} reducers. As this ratio diverges between treatments with depth, it provides further evidence for the existence of this separate "NO_3^--accessible" OM pool that microbes can access once NO_3^- limitation is released. There are other processes by which this increasing pattern in DIC:NH_4^+ can emerge, including differences in microbial biomass and N uptake or anammox (Dalsgaard, Thamdrup, & Canfield, 2005; Schmid et al., 2007). Our NH_4^+ data seem to suggest, however, that there was not significant differences in uptake or regeneration between treatments, given that cumulative NH_4^+ production across the entire experiment was the same (Fig. 5). Further, we have stable isotope $^{29}N_2$ production data (Bulseco-McKim et al., 2018) showing that anammox was negligible in this experiment, agreeing with other studies conducted in salt marsh sediments (Koop-Jakobsen & Giblin, 2009). We therefore conclude that this increase in DIC:NH_4^+ ratio may be explained, at least in part, by the oxidation of a higher C/N pool of OM at depth in the plus-NO_3^- treatment.

514 FT-IR spectral data also suggest that microbes in the plus-NO_3^- treatment were accessing
515 a different pool of OM. A PCoA of the whole FT-IR spectra from 4000-400 cm^{-1} indicated a
516 significant difference in the OM chemistry among treatments and depth (Fig. 7A). This result
517 suggests that decomposition not only caused a shift in the OM signature when compared to pre-
518 sediments, but also, that the plus-NO_3^- and unamended OM composition shifted in different
519 ways. In addition, higher Index II values in both the plus-NO_3^- and unamended treatments
520 compared to the pre-sediments show that microbial OM oxidation resulted in more recalcitrant
521 OM (Fig. 7C), a result that we could not detect in the bulk sediment properties (Table 2).
522 Remarkably, these data also suggest that after incubation, the OM from the unamended
523 treatments is more recalcitrant than the OM from the plus-NO_3^- treatment (Fig. 7C). One possible
524 explanation for this counterintuitive finding is that NO_3^- addition might be facilitating
525 decomposition of more complex OM (e.g. large cyclic compounds such as cellulose), either
526 through fermentation or hydrolysis, which would result in more labile, low-molecular-weight
527 substrates (Beauchamp, Trevors, & Paul,1989). Rather than a predictable sequence following
528 thermodynamic theory, which asserts that electron acceptors with higher redox potential are
529 exclusively reduced first (Zehnder & Stumm, 1988), these results suggest that NO_3^- supports co-
530 metabolism by providing more labile OM compounds for competing microbial functional groups
531 (Achtnich et al., 1995). In the unamended treatment, SO_4^{2-} reducers may only have access to a
532 limited supply of low-molecular-weight substrates (Canfield et al., 2005), therefore creating a
533 more recalcitrant OM pool over time (Fig. 1, 3). Similar results have been observed in both
534 terrestrial and oceanic studies, with N addition resulting in the selection for N-derived microbes
535 that could decompose recalcitrant carbon compounds more efficiently (Allison et al., 2013;
536 Campbell, Polson, Hanson, Mack, & Schuur, 2010; Treseder et al., 2011). Another possible

explanation for a more labile signature in the plus-NO_3^- treatment is a greater supply of extracellular DNA from greater microbial biomass (e.g. Dell'Anno & Danavaro, 2005), however since NH_4^+ production rates were similar between treatments (Fig. 5), this is likely not the case. While we did not explicitly test this hypothesis, it does provide one potential mechanism that could be explored through further experimentation.

4.3. NO_3^- addition effects on microbial community structure

We hypothesized that the end result of NO_3^- addition would be 1) to fundamentally alter the resident microbial community through a change in the competitive landscape or 2) to alter the function of the existing community through metabolic plasticity of the microbes present (Allison & Martiny, 2008), with both scenarios resulting in shifts in the dominant metabolic pathways. Through 16S rRNA gene sequencing, we found evidence for a combination of the two. While we observed a core microbiome that existed in both the plus-NO_3^- and unamended treatment (Fig. S3), including microbial taxa typically present in these particular salt marsh sediments (e.g. Kearns et al., 2016), we also found a significant shift in microbial community structure (Fig. 8A) and decreases in alpha diversity (Fig. 8B) in response to NO_3^-. This suggests that NO_3^- addition selects for taxa that are more competitive in a high N environment, and that this community is fundamentally different from both pre- and unamended sediments.

Through random forest classification analysis, we identified 30 ASVs most important in correctly classifying between plus-NO_3^- and unamended treatments (Fig. 9; Table S2). Out of these 30 ASVs, ~70% were from the class Gammaproteobacteria, a widely diverse group of gram-negative bacteria that increase in abundance as a result of fertilization (e.g. Campbell et al., 2010). Many of these ASVs were putatively assigned to orders known to reduce nitrate

(Kiloniellales; Wiese, Thiel, Gärtner, Schmaljohann, & Imhoff, 2009) oxidize sulfur/sulfide (Thiotrichales, Chromatiales; Garrity, Bell, & Lilburn, 2005; Imhoff, 2005; Thomas, Giblin, Cardon, & Sievert, 2014), ferment OM (Ignavibacteriales, Rhodospirallales; (Biebl & Pfening, 1981; Iino et al., 2010), and degrade high-molecular-weight (HMW) compounds (Flavobacteriales, Thiotrichales, Alteromonadales). Some members of these groups can also use long-chain alkanes (Fernández-Gómez et al., 2013; Guibert et al., 2016) and are stimulated in the presence of HMW dissolved organic matter (Mahmoudi et al., 2015; McCarren et al., 2010). These shifts in the community provide evidence for selection of taxa more adept at using nitrate or oxidizing more complex OM. In contrast, ASVs more abundant in the unamended treatment included orders that are ubiquitous in soil and mangrove sediments (Verrucomicrobiae, Caldithrixales; (Freitas et al., 2012; Miroshnichenko, Kolganova, Spring, Chernyh, & Bonch-Osmolovskaya, 2010), that can reduce sulfate (Desulfobacterales, Desulfarculales; Bahr et al., 2005), and that exhibit properties associated with iron metabolism (Campylobacterales, Rhizobiales (Eppinger, Baar, Raddatz, Huson, & Schuster, 2004; Reese, Witmer, Moller, Morse, & Mills, 2013). While we cannot make definitive statements regarding the exact function associated with these taxa, identifying the taxa most responsive to NO_3^- addition is a step forward in understanding the mechanistic response of microbial communities to nutrient enrichment.

4.4. Assumptions and limitations of FTR experiments

We chose a high concentration of NO_3^- (500 µM NO_3^-) to assure non-limiting concentrations at a reasonable flow rate (Pallud et al., 2007). We designed this experiment specifically to assess the potential of NO_3^- to mobilize carbon pools that were not being oxidized by SO_4^{2-} reduction, rather than to simulate realistic environmental conditions. In the

environment, NO_3^- will almost always be limiting except in the most eutrophic conditions or in situations of continuous replacement. Further, the use of FTRs eliminates the complexity involved with plant-microbe feedbacks and competition for NO_3^- by benthic microalgae and phytoplankton. While these interactions are important, the aim of this experiment was to directly assess microbial processes. We also assumed that in our experiment, SO_4^{2-} was the only electron acceptor being supplied in our unamended treatment aside from the very small background concentration of NO_3^- (0.6-1.2 μM) in the seawater we used. We do not believe that this affected the treatment differences. Since background SO_4^{2-} concentrations are so high in seawater (~28 mM), we were not able to detect small changes at the μM level that occurred in the FTRs and had to instead infer SRR from rates of sulfide production and changes in sediment S concentrations. These changes are likely due to pyrite or FeS formation; although we cannot rule out the production of organic sulfur (Luther III, Church, Scudlark, & Cosman, 1986). Although we did not monitor the influent oxygen concentrations, we conducted the entire experiment in an anoxic glove chamber, so oxygen should not have been present for either oxic respiration or nitrification. In both treatments, iron oxides were likely available, especially in the shallow sediments, which may have contributed to DIC production; however, since both treatments started with the same sediments, the initial iron concentration should be comparable between the two. Finally, since this experiment only lasted ~90 days, we cannot determine how large the NO_3^--accessible OM pool is, whether NO_3^- reducers are solely responsible for the stimulation, or if they also stimulate SO_4^{2-} reducers through co-metabolism.

Extrapolating to the ecosystem-level from small-scale laboratory experiments is challenging; but these FTRs are specifically designed to isolate meaningful parameters and to allow for the extraction of kinetic rate measurements of specific microbial processes, which can

606 then be used to inform predictive models designed for unraveling sediment biogeochemistry
607 across various spatial and temporal scales (see Algar & Vallino, 2014; Vallino, 2011).
608
609 *4.5. Implications of N-loading on salt marsh carbon storage capacity*
610 Our results show that NO_3^- addition stimulates DIC production and consequently,
611 decomposition of OM in salt marsh sediments. We observed this response even in deep
612 sediments, where we traditionally assume OM to be fairly recalcitrant to microbial degradation.
613 We hypothesize that by adding NO_3^- and providing a more energetically favorable electron
614 acceptor to the system, we are shifting the microbial community towards taxa better suited for a
615 high NO_3^- environment, and consequently changing the accessible OM pool from one that is
616 stable and recalcitrant to SO_4^{2-} reducers, to one that is bioavailable under high NO_3^- conditions.
617 These results suggest that comparable additions of NO_3^- to salt marshes could enhance OM
618 decomposition *in situ.*
619 These results could have important implications for salt marsh carbon storage potential.
620 The effect of adding NO_3^- that we demonstrate here, would depend on the specific hydrology of
621 the marsh system. If NO_3^- -rich flooding waters penetrate into deep sediments, it could accelerate
622 decomposition of stored carbon. Not only could this decrease carbon storage potential, it could
623 also result in decreased belowground marsh stability (e.g. Deegan et al., 2012) and lead to
624 greater CO_2 production. Additionally, marsh systems currently experiencing high NO_3^-
625 conditions may store less OM over time, leading to less overall carbon storage; although the OM
626 that is buried may be more recalcitrant, since a larger portion will already be oxidized. What this
627 means for carbon storage potential of marshes at a larger scale is unclear, since NO_3^- can also
628 stimulate OM production by acting as a nutrient, with such production offsetting respiration.

Total marsh carbon storage capacity depends heavily on the balance between these two processes. Considering the degree of eutrophication in US estuaries (Bricker et al., 2008), and how NO_3^- addition alters processes that control OM, it is important to incorporate our understanding of these processes when assessing the resilience of salt marsh systems to changing climate and increasing anthropogenic pressures. This is especially critical if we hope to rely on salt marshes for long-term carbon storage.

Acknowledgements

We would like to thank Joseph Vallino at Marine Biological Laboratory for his invaluable contribution to the design of our flow through reactor system. We also thank researchers of the TIDE project (NSF OCE0924287, OCE0923689, DEB0213767, DEB1354494, and OCE 1353140) for maintenance of the long-term nutrient enrichment experiment, as well as researchers of the Plum Island Ecosystems LTER (NSF OCE 0423565, 1058747, 1637630). We would also like to acknowledge Sam Kelsey, Khang Tran, Michael Greenwood, and members of the Bowen lab for their assistance in the field and laboratory, as well as Inke Forbrich, Nat Weston, and Gary Banta for their thoughtful comments on this research. This work was funded by an NSF CAREER Award to JLB (DEB1350491) and a Woods Hole Oceanographic Sea Grant award to AEG and JJV (Project No. NA140AR4170074 Project R/M-65s). Additional support was provided by a Ford Foundation pre-doctoral fellowship award to ABM. All sequence data from this study is available in the Sequence Read Archive under accession number TBD. The views expressed here are those of the authors and do not necessarily reflect the views of NOAA or any of is sub-agencies.

References

Achtnich, C., Bak, F., & Conrad, R. (1995). Competition for electron donors among nitrate reducers, ferric iron reducers, sulfate reducers, and methanogens in anoxic paddy soil. *Biology and Fertility of Soils*, *19*, 65–72.

Algar, C. K., & Vallino, J. J. (2014). Predicting microbial nitrate reduction pathways in coastal sediments. *Aquatic Microbial Ecology*, *71*, 223–238.

Aller, R. C., & Aller, J. Y. (1998). The effect of biogenic irrigation intensity and solute exchange on diagenetic reaction rates in marine sediments. *Journal of Marine Research, 56*, 905–936.

Allison, S. D., Lu, Y., Weihe, C., Goulden, M.L., Martiny, A.C., Treseder, K. K., & Martiny, J. B. H. (2013). Microbial abundance and composition influence litter decomposition response to environmental change. *Ecology*, *94*, 714–725.

Allison, S. D., & Martiny, J. B. H. (2008). Resistance, resilience, and redundancy in microbial communities. *Proceedings of the National Academy of Sciences of the United States of America*, *105*, 11512-11519.

Apprill, A., Mcnally, S., Parsons, R., & Weber, L. (2015). Minor revision to V4 region SSU rRNA 806R gene primer greatly increases detection of SAR11 bacterioplankton. *Aquatic Microbial Ecology*, *75*, 129–137.

Arndt, S., Jørgensen, B. B., LaRowe, D. E., Middelburg, J. J., Pancost, R. D., Regnier, P. (2013) Quantifying the degradation of organic matter in marine sediments: A review and synthesis. *Earth-Science Reviews*, *123*, 53–86.

Artz, R. R. E., Chapman, S. J., Robertson, A.H., Potts, J.M., Laggoun-Défarge, F., Gogo, S., … & Francez, A. (2008). FTIR spectroscopy can predict organic matter quality in regenerating cutover peatlands. *Soil Biology and Biochemistry*, *40*, 515–527.

675 Bahr, M., Crump, B. C., Klepac-Ceraj, V., Teske, A., Sogin, M. L., & Hobbie, J. E. (2005).
676 Molecular characterization of sulfate-reducing bacteria in a New England salt marsh.
677 *Environmental Microbiology*, *7*, 1175–85.
678 Beauchamp, E., Trevors, J., & Paul, J. W. (1989). Carbon sources for bacterial denitrification.
679 *Advances in Soil Science*, *10*, 113–142.
680 Benner, R., Newell, S. Y., Maccubbin, A. E., & Hodson, R. E. (1984). Relative contributions of
681 bacteria and fungi to rates of degradation of lignocellulosic detritus in salt-marsh sediments.
682 *Applied and Environmental Microbiology*, *48*, 36–40.
683 Biebl, H., & Pfening, N. (1981). Isolation of members of the family Rhodospirillaceae. In M.
684 Starr, H. Stolp, H. Truper, A. Balows, & H. Schlegel (Eds.), *The Prokaryotes* (pp. 267–
685 268). Berlin: Springer Berlin Heidelberg.
686 Bricker, S. B., Longstaff, B., Dennison, W., Jones, A., Boicourt, K., Wicks, C., & Woerner, J.
687 (2008). Effects of nutrient enrichment in the nation's estuaries: A decade of change.
688 *Harmful Algae*, *8*, 21–32.
689 Bulseco-McKim, A. (2018) The role of nitrate in salt marsh sediment organic matter
690 decomposition (PhD thesis). Retrieved from ProQuest Disserations and Theses database.
691 Callahan, B. J., McMurdie, P. J., Rosen, M. J., Han, A.W., Johnson, A. J. A., & Holmes, S. P.
692 (2016). DADA2: High-resolution sample inference from Illumina amplicon data. *Nature*
693 *Methods*, *13*, 581–583.
694 Campbell, B. J., Polson, S. W., Hanson, T. E., Mack, M. C., & Schuur, E. A. G. (2010). The
695 effect of nutrient deposition on bacterial communities in Arctic tundra soil. *Environmental*
696 *Microbiology*, *12*, 1842–1854.
697 Canfield D. (1989) Sulfate reduction and oxic respiration in marine sediments: implications for

698 organic carbon preservation in euxinic environments. *Deep Sea Research Part A:*
699 *Oceanogorahic Research Papers, 36*, 121–138.
700 Canfield, D. E., & Farquhar, J. (2009). Animal evolution , bioturbation , and the sulfate
701 concentration of the oceans. *Proceedings of the National Academy of Sciences*, *106*, 8123-
702 8127.
703 Canfield, D. E., Thamdrup, B., & Kristensen, E. (2005). *Aquatic Geomicrobiology*. (A. J.
704 Southward, P. A. Tyler, C. M. Young, & L. A. Fuiman, Eds.). Boston, MA: Elsevier
705 Academic Press.
706 Caporaso, J. G., Lauber, C. L., Walters, W. A., Berg-Lyons, D., Lozupone, C. A., Turnbaugh, P.
707 J., … Knight, R. (2011). Global patterns of 16S rRNA diversity at a depth of millions of
708 sequences per sample. *Proceedings of the National Academy of Sciences,108*, 4516-4522.
709 Caporaso, J. G., Lauber, C. L., Walters, W. a, Berg-Lyons, D., Huntley, J., Fierer, N., … Knight,
710 R. (2012). Ultra-high-throughput microbial community analysis on the Illumina HiSeq and
711 MiSeq platforms. *The ISME Journal*, *6*, 1621–1624.
712 Chmura, G. L., Anisfeld, S. C., Cahoon, D. R., & Lynch, J. C. (2003). Global carbon
713 sequestration in tidal, saline wetland soils. *Global Biogeochemical Cycles*, *17*, 1-12.
714 Cox, R.D. (1980). Determination of nitrate and nitrite at the parts per billion level by
715 chemiluminescence. *Analytical Chemistry*, *52,* 332-335.
716 Dalsgaard, T., Thamdrup, B., & Canfield, D. E. (2005). Anaerobic ammonium oxidation
717 (anammox) in the marine environment. *Research in Microbiology*, *156*, 457–64.
718 Dargusch, P., & Thomas, S. (2012). A critical role for carbon offsets. *Nature Climate Change*, *2*,
719 470–470.
720 Deegan, L. A., Johnson, D. S., Warren, R. S., Peterson, B. J., Fleeger, J. W., Fagherazzi, S., &

721 Wollheim, W. M. (2012). Coastal eutrophication as a driver of salt marsh loss. *Nature*, *490*,
722 388–392.
723 Deegan, L. A., Bowen, J. L., Drake, D., Fleeger, J. W., Friedrichs, C. T., Galván, K. A, … &
724 Hopkinson, C. (2007). Susceptibility of salt marshes to nutrient enrichment and predation
725 removal. *Ecological Applications*, *17*, 42–63.
726 Dell'Anno, A., & Danavaro, R. (2005). Extracellular DNA plays a key role in deep-sea
727 ecosystem functioning. *Science*, *309*, 2179–2179.
728 Dickson, A.G., Goyet, C. (1994) Handbook of methods for the analysis of various parameters of
729 the carbon dioxide system in sea water; version 2. DOE ORNL/CDIAC 74.
730 Ding, G., Novak, J. M., Amarasiriwardena, D., Hunt, P. G., & Xing, B. (2002). Soil Organic
731 Matter Characteristics as Affected by Tillage Management. *Soil Science Society of America*
732 *Journal*, *66*, 421-429.
733 Duarte, C. M., Middelburg, J. J., & Caraco, N. (2005). Major role of marine vegetation on the
734 oceanic carbon cycle. *Biogeosciences*, *2*, 1-8.
735 Eppinger, M., Baar, C., Raddatz, G., Huson, D. H., & Schuster, S. C. (2004). Comparative
736 analysis of four campylobacterales. *Nature Reviews Microbiology*, *2*, 872–885.
737 Falkowski, P. G., Fenchel, T., & Delong, E. F. (2008). The microbial engines that drive Earth's
738 biogeochemical cycles. *Science*, *320*, 1034-1039.
739 Fernández-Gómez, B., Richter, M., Schüler, M., Pinhassi, J., Acinas, S. G., González, J. M., &
740 Pedrós-Alió, C. (2013). Ecology of marine bacteroidetes: A comparative genomics
741 approach. *The ISME Journal*, *7*, 1026–1037.
742 Forbrich, I., Giblin, A. E., & Hopkinson, C. S. (2018) Constraining marsh carbon budgets using
743 long-term C burial and contemporary atmospheric CO2 fluxes. *Journal of Geophysical*

744 *Research: Biogeosciences*, 123, 867-878.
745 Freitas, S., Hatosy, S., Fuhrman, J. A., Huse, S. M., Mark Welch, D. B., Sogin, M. L., &
746 Martiny, A. C. (2012). Global distribution and diversity of marine Verrucomicrobia. *The*
747 *ISME Journal*, *6*, 1499–1505.
748 Froelich, P., Klinkhammer, G., Bender, M., Luedtke, N., Heath, G., Cullen, D., & Dauphin, P.
749 (1979). Early oxidation of organic matter in pelagic sediments of the eastern equatorial
750 Atlantic: suboxic diagenesis. *Geochimica et Cosmochimica Acta*, *43*, 1075–1090.
751 Galloway, J. N., Leach, A. M., Erisman, J. W., & Bleeker, A. (2017). Nitrogen the historical
752 progression from ignorance to knowledge with a view to future solutions. *Soil Research*, *55*,
753 417–424.
754 Galloway, J. N., Townsend, A. R., Erisman, J. W., Bekunda, M., Cai, Z., Freney, J. R., … &
755 Sutton, M. A. (2008). Transformation of the Nitrogen Cycle : Recent Trends, Questions,
756 and Potential Solutions. *Science*, *320*, 889-892.
757 Garrity, G., Bell, J., & Lilburn, T. (2005). Thiotrichales ord. nov. In D. Brenner (Ed.), *Bergey's*
758 *Manual of Systematic Bacteriology* (2nd ed.). Boston, MA.
759 Giblin, A., Tobias, C., Song, B., Weston, N., Banta, G., & Rivera-Monroy, V. (2013). The
760 Importance of Dissimilatory Nitrate Reduction to Ammonium (DNRA) in the Nitrogen
761 Cycle of Coastal Ecosystems. *Oceanography*, *26*, 124–131.
762 Gilboa-Garber, N. (1971). Direct spectrophotometric determination of inorganic sulfide in
763 biological materials and in other complex mixtures. *Analytical Biochemistry*, *43*, 129–133.
764 Giovannoni, S. J. (2017). SAR11 Bacteria: The Most Abundant Plankton in the Oceans. *Annual*
765 *Review of Marine Science*, *9*, 231–255.
766 Guibert, L. M., Loviso, C. L., Borglin, S., Jansson, J. K., Dionisi, H. M., & Lozada, M. (2016).

Diverse Bacterial Groups Contribute to the Alkane Degradation Potential of Chronically Polluted Subantarctic Coastal Sediments. *Microbial Ecology*, *71*, 100–112.

Hamersley, M. R., & Howes, B. L. (2005). Coupled nitrification-denitrification measured *in situ* in a Spartina alterniflora marsh with a $^{15}NH_4^+$ tracer. *Marine Ecology Progress Series*, *299*, 123–135.

Hedges, J. I., Eglinton, G., Hatcher, P. G., Kirchman, D. L., Arnosti, C., Derenne, S., … & Rullkötter, J. (2000). The molecularly uncharacter ized component of nonliving organic matter in natural environments. *Organic Geochemistry*, *31*, 945–958.

Hopkinson, C. S., & Giblin, A. E. (2008). Nitrogen dynamics of coastal salt marshes. In D. Capone, D. Bronk, M. Mulholland, & E. Carpenter (Eds.), *Nitrogen in the Marine Environment* (2nd ed., pp. 991–1036). Burlington, MA: Academic Press.

Howarth, R. W. (1984). The ecological significance of sulfur in the energy dynamics of salt marsh and coastal marine sediments. *Biogeochemistry*, *1*, 5-27.

Howarth, R. W., & Teal, J. M. (1979). Sulfate reduction in a New England salt marsh. *Limnology and Oceanography*, *24*, 999–1013.

Howes, B. L., Howarth, R. W., Teal, J. M., & Valiela, I. (1981). Oxidation-reduction potentials in a salt marsh: Spatial patterns and interactions with primary production. *Limnology and Oceanography*, *26*, 350-360.

Iino, T., Mori, K., Uchino, Y., Nakagawa, T., Harayama, S., & Suzuki, K. I. (2010). *Ignavibacterium album* gen. nov., sp. nov., a moderately thermophilic anaerobic bacterium isolated from microbial mats at a terrestrial hot spring and proposal of Ignavibacteria classis nov., for a novel lineage at the periphery of green sulfur bacteria. *International Journal of Systematic and Evolutionary Microbiology*, *60*, 1376–1382.

790 Imhoff, J. (2005). Bergey's Manual of Systematic Bacteriology. In D. Brenner, N. Krieg, J.
791 Staley, & G. Garrity (Eds.), *Bergey's Manual of Systematic Bacteriology* (2nd ed.). New
792 York, NY.
793 Jørgensen, B. B. (1977). The sulfur cycle of a coastal marine sediment (Limfjorden, Denmark).
794 *Limnology and Oceanography*, *22*, 814-832.
795 Kaplan, W., Valiela, I., & Teal, J. M. (1979). Denitrification in a salt marsh ecosystem.
796 *Limnology and Oceanography*, *24*, 726–734.
797 Katoh, K., & Standley, D. M. (2013). MAFFT multiple sequence alignment software version 7:
798 Improvements in performance and usability. *Molecular Biology and Evolution*, *30*, 772–
799 780.
800 Kearns, P. J., Angell, J. H., Howard, E., Deegan, L. A., Stanley, R. H., & Bowen, J. L. (2016).
801 Nutrient enrichment induces high rates of dormancy and decreases diversity of active
802 bacterial taxa. *Nature Communications*, *7*, 1–9.
803 Koop-Jakobsen, K., & Giblin, A. E. (2009). Anammox in tidal marsh sediments: The role of
804 salinity, nitrogen loading, and marsh vegetation. *Estuaries and Coasts*, *32*, 238–245.
805 Koop-Jakobsen, K., & Giblin, A. E. (2010). The effect of increased nitrate loading on nitrate
806 reduction via denitrification and DNRA in salt marsh sediments. *Limnology and*
807 *Oceanography*, *55*, 789–802.
808 Kostka, J. E., Gribsholt, B., Petrie, E., Dalton, D., Skelton, H., & Kristensen, E. (2002). The rates
809 and pathways of carbon oxidation in bioturbated saltmarsh sediments. *Limnology and*
810 *Oceanography*, *47*, 230–240.
811 Kuhn, M. (2016). A Short Introduction to the caret Package. *R Foundation for Statistical*
812 *Computing*, 1–10. Retrieved from cran.r-project. org/web/packages/caret/vignettes/caret.pdf

Langley, J. A., Mozdzer, T. J., Shepard, K. A., Hagerty, S. B., & Megonigal, J. P. (2013) Tidal marsh plant responses to elevated CO_2, nitrogen fertilization, and sea level rise. *Global Change Biology*, *19*, 1495-1503.

Liaw, A., & Wiener, M. (2002). Classification and Regression by randomForest. *R News*, 2, 18-22.

Lozupone, C., Lladser, M. E., Knights, D., Stombaugh, J., & Knight, R. (2011). UniFrac: An effective distance metric for microbial community comparison. *The ISME Journal*, *5*, 169–172.

Luther III, G., Church, T. M., Scudlark, J. R., & Cosman, M. (1986). Inorganic and Organic Sulfur Cycling in Salt-Marsh Pore Waters, *Science*, *232*, 746–749.

Macreadie, P. I., Nielsen, D. A., Kelleway, J. J., Atwood, T. B., Seymour, J. R., Petrou, K., … & Ralph, P. J. (2017). Can we manage coastal ecosystems to sequester more blue carbon? *Frontiers in Ecology and the Environment*, *15*, 206–213.

Mahmoudi, N., Robeson II, M. S., Castro, H. F., Fortney, J. L., Techtmann, S. M., Joyner, D. C., …& Hazen, T. C. (2015). Microbial community composition and diversity in Caspian Sea sediments. *FEMS Microbiology Ecology*, *91*, 1–11.

Margenot, A. J., Calderón, F. J., Bowles, T. M., Parikh, S. J., & Jackson, L. E. (2015). Soil Organic Matter Functional Group Composition in Relation to Organic Carbon, Nitrogen, and Phosphorus Fractions in Organically Managed Tomato Fields. *Soil Science Society of America Journal*, *79*, 772–782.

McCarren, J., Becker, J. W., Repeta, D. J., Shi, Y., Young, C. R., Malmstrom, R. R., … & DeLong, E. F. (2010). Microbial community transcriptomes reveal microbes and metabolic pathways associated with dissolved organic matter turnover in the sea. *Proceedings of the*

836 *National Academy of Sciences*, *107*, 16420–16427.
837 McDonald, D., Price, M. N., Goodrich, J., Nawrocki, E. P., Desantis, T. Z., Probst, A., … &
838 Hugenholtz, P. (2012). An improved Greengenes taxonomy with explicit ranks for
839 ecological and evolutionary analyses of bacteria and archaea. *ISME Journal*, *6*, 610–618.
840 Mcleod, E., Chmura, G. L., Bouillon, S., Salm, R., Björk, M., Duarte, C. M., … & Silliman, B.
841 R. (2011). A blueprint for blue carbon: toward an improved understanding of the role of
842 vegetated coastal habitats in sequestering CO 2. *Frontiers in Ecology and the Environment*,
843 *9*, 552–560.
844 Meyer, A. F., Lipson, D. A., Martin, A. P., Schadt, C. W., & Schmidt, S. K. (2004). Molecular
845 and Metabolic Characterization of Cold-Tolerant Alpine Soil Pseudomonas Sensu Stricto.
846 *Applied and Environmental Microbiology*, *70*, 483–489.
847 Miroshnichenko, M. L., Kolganova, T. V., Spring, S., Chernyh, N., & Bonch-Osmolovskaya, E.
848 A. (2010). Caldithrix palaeochoryensis sp. nov., a thermophilic, anaerobic, chemo-
849 organotrophic bacterium from a geothermally heated sediment, and emended description of
850 the genus Caldithrix. *International Journal of Systematic and Evolutionary Microbiology*,
851 *60*, 2120–2123.
852 Morris, J. T., Sundareshwar, P. V., Nietch, C. T., Kjerfve, B., & Cahoon, D. R. (2002).
853 Responses of coastal wetlands to rising sea level. *Ecology*, *83*, 2869–2877.
854 Nelleman, C., Corcoran, E., Duarte, C., Valdes, L., De Young, C., Foncesa, L., & Grimsditch, G.
855 (2009). Blue carbon: A rapid response assessment. *Arendal Norway: United Nations*
856 *Environment Programme.*
857 Pallud, C., Meile, C., Laverman, A. M., Abell, J., & Van Cappellen, P. (2007). The use of flow-
858 through sediment reactors in biogeochemical kinetics: Methodology and examples of

applications. *Marine Chemistry*, *106*, 256–271.

Pallud, C., & Van Cappellen, P. (2006). Kinetics of microbial sulfate reduction in estuarine sediments. *Geochimica et Cosmochimica Acta*, *70*, 1148–1162.

Parikh, S. J., Goyne, K. W., Margenot, A. J., Mukome, F. N. D., & Calderón, F. J. (2014). Soil chemical insights provided through vibrational spectroscopy. In *Advances in Agronomy* (Vol. 126, pp. 1-148). Academic Press.

Pastore, M.A, Megonigal, J.P., & Langley, J.A. (2017) Elevated CO_2 and nitrogen addition accelerate net carbon gain in a brackish marsh. *Biogeochemistry*, *133*,73-87.

Reddy, K., & Patrick Jr., W. (1975). Effect of alternate aerobic and anaerobic conditions on redox potential, organic matter decomposition, and nitrogen loss in a flooded soil. *Soil Biology and Biochemistry*, *7*, 87–94.

Reese, B. K., Witmer, A. D., Moller, S., Morse, J. W., & Mills, H. J. (2013). Molecular assays advance understanding of sulfate reduction despite cryptic cycles. *Biogeochemistry*, *118*, 307–319.

Ryther, J. H., & Dunstan, W. M. (1971). Nitrogen , Phosphorus , and Eutrophication in the Coastal Marine Environment. *Science*, *171*, 1008–1013.

Schmid, M. C., Risgaard-Petersen, N., Van De Vossenberg, J., Kuypers, M. M. M., Lavik, G., Petersen, J., … & Jetten, M. S. M. (2007). Anaerobic ammonium-oxidizing bacteria in marine environments: Widespread occurrence but low diversity. *Environmental Microbiology*, *9*, 1476–1484.

Shade, A., Peter, H., Allison, S. D., Baho, D. L., Berga, M., Bürgmann, H., … & Handelsman, J. (2012). Fundamentals of microbial community resistance and resilience. *Frontiers in Microbiology*, *3*, 1–19.

882 Solórzano, L. (1969) Determination of ammonia in natural waters by the phenolhypochlorite
883 method. *Limnology and Oceanography*, *14*, 799-801.
884 Thamdrup, B., & Dalsgaard, T. (2002). Production of N_2 through anaerobic ammonium
885 oxidation coupled to nitrate reduction in marine sediments. *Applied and Environmental*
886 *Microbiology*, *68*, 1312–1318.
887 Thomas, F., Giblin, A. E., Cardon, Z. G., & Sievert, S. M. (2014). Rhizosphere heterogeneity
888 shapes abundance and activity of sulfur-oxidizing bacteria in vegetated salt marsh
889 sediments. *Frontiers in Microbiology*, *5*, 309.
890 Treseder, K. K., Kivlin, S. N., & Hawkes, C. V. (2011). Evolutionary trade-offs among
891 decomposers determine responses to nitrogen enrichment. *Ecology Letters*, *14*, 933–938.
892 Valiela, I., & Cole, M. L. (2002). Comparative evidence that salt marshes and mangroves may
893 protect seagrass meadows from land-derived nitrogen loads. *Ecosystems*, *5*, 92–102.
894 Valiela, I., & Teal, J. M. (1974). Nutrient limitation in salt marsh vegetation. In R. J. Reimold &
895 W. H. Queen (Eds.), *Ecology of Halophytes* (pp. 547–563). New York, NY: Academic
896 Press.
897 Vallino, J. J. (2011). Differences and implications in biogeochemistry from maximizing entropy
898 production locally versus globally. *Earth System Dynamics*, *2*, 69–85.
899 Veum, K. S., Goyne, K. W., Kremer, R. J., Miles, R. J., & Sudduth, K. A. (2014). Biological
900 indicators of soil quality and soil organic matter characteristics in an agricultural
901 management continuum. *Biogeochemistry*, *117*, 81–99.
902 Vivanco, L, Irvine, I.C., & Martiny, J.B.H. (2015) Nonlinear responses in salt marsh functioning
903 to increased nitrogen addition. *Ecology, 96,* 936-947.
904 Warren, R. S., Fell, P. E., Rozsa, R., Brawley, A. H., Orsted, A. C., Olson, E. T., … & Niering,

W. A. (2002). Salt marsh restoration in Connecticut: 20 years of science and management. *Restoration Ecology*, *10*, 497–513.

Westrich, J. T., & Berner, R. A. (1984). The role of sedimentary organic matter in bacterial sulfate reduction: The G model tested. *Limnology and Oceanography*, *29*, 236–249.

Wieder, W. R., Bonan, G. B., & Allison, S. D. (2013). Global soil carbon projections are improved by modelling microbial processes. *Nature Climate Change*, *3*, 909–912.

Wiese, J., Thiel, V., Gärtner, A., Schmaljohann, R., & Imhoff, J. F. (2009). Kiloniella laminariae gen. nov., sp. nov., an alphaproteobacterium from the marine macroalga Laminaria saccharina. *International Journal of Systematic and Evolutionary Microbiology*, *59*, 350–356.

Wilson, C. A., Hughes, Z. J., FitzGerald, D. M., Hopkinson, C. S., Valentine, V., & Kolker, A. S. (2014) Saltmarsh pool and tidal creek morphodynamics: Dynamic equilibrium of northern latitude saltmarshes? *Geomorphology*, *213*, 99–115.

Zehnder A, Stumm W (1988) Geochemistry and biogeochemistry of anaerobic habitats. In: Zehnder A (ed) Biology of Anaerobic Microorganisms. Wiley, p 1–38.